Chemistry & Biology 13, 123–128, February 2006 ©2006 Elsevier Ltd All rights reserved DOI 10.1016/j.chembiol.2005.12.013

Stereoisomers of *P. aeruginosa* Autoinducer Analog to Probe the Regulator Binding Site

Brief Communication

Geetanjali J. Jog,[1] Jun Igarashi,[2] and Hiroaki Suga[1,2,*]
[1] Department of Chemistry
State University of New York at Buffalo
Buffalo, New York 14260
[2] Research Center for Advanced Science and Technology
University of Tokyo
4-6-1 Komaba
Meguro-ku
Tokyo, 153-8904
Japan

Summary

Quorum sensing (QS) regulates the production of virulence factors and the maturation of biofilms in many bacteria, including *Pseudomonas aeruginosa*. The QS cascade is activated by the interaction of bacterial signaling molecules, called autoinducers (AIs), with their corresponding regulatory proteins. Here, we report a series of studies to define the stereochemical preferences of synthetic agonists and perform docking studies to understand the microenvironment of the binding site in *P. aeruginosa* QS regulators. One of the key findings of this work is that the ring structure and the absolute and relative stereochemistries of the amide and hydroxyl groups dictate the agonist activity. This study aids in determining important structural and stereochemical characteristics necessary for interaction with the QS regulatory proteins, thus expanding our understanding of their inducer binding sites.

Introduction

Pseudomonas aeruginosa is an opportunistic pathogen and is a common cause of infections in immunocompromised individuals and individuals with cystic fibrosis [1]. Expression of genes that produce virulence factors such as alkaline protease, elastase, exotoxin A, rhamnolipids, and pyocyanin is governed by the response to the cell density that is monitored by a mechanism known as quorum sensing (QS) [2–5]. Biofilm formation is also a major contributor to the virulence causing persistent infections in lungs of cystic fibrosis patients, in which the regulation of mature biofilm formation is also linked to the QS mechanism [6]. In *P. aeruginosa*, QS consists of two separate cascades, *las* and *rhl*, consisting of regulatory (R) proteins, LasR and RhlR, and inducer (I) proteins, LasI and RhlI, respectively. The I proteins synthesize the corresponding signaling molecules (called autoinducers [AIs]), *N*-(3-oxododecanoyl)-L-homoserine lactone ($3OC_{12}$-L-HSL), and *N*-butanoyl-L-homoserine lactone (C_4-L-HSL), and these molecules bind the cognate R proteins to activate the QS circuits (Figure 1A, X = L-HSL) [7, 8]. There exists a regulation hierarchy within this QS system in which the LasR-$3OC_{12}$-L-HSL complex regulates *rhlR* expression [9]. Since QS plays a central role in governing the gene expression of various virulence factors, controlling QS by means of interfering with the binding of AIs with their respective R proteins potentially offers a curative form of treatment [10–13].

To gain insights into the molecular interaction of the AIs with their cognate R proteins and ultimately aid rational design of QS inhibitors, a study encompassing synthesis and testing of a library of AI analogs was performed earlier in our laboratory [14–16]. Our approach for designing the AI library involved substitution of the HSL moiety, which is a common structural element of AIs in many gram-negative bacteria, with various amines. Our study has identified several hits that act as agonist or antagonist for the *P. aeruginosa* QS circuits. Among them, the $3OC_{12}$ derivative of *trans*-2-aminocyclohexanol (*rac*-**1**, in Figure 1B) effectively agonizes the *las* circuit, whereas the C_4 derivatives of *trans*-2-aminocyclohexanone (*rac*-**3**) and *trans*-2-aminocyclopentanone (*rac*-**4**) agonize the *rhl* circuit more so than that of *rac*-**1**. Interestingly, neither the $3OC_{12}$ nor C_4 AI analog containing the substitution of *trans*-2-aminocyclopentanol (*rac*-**2**, Figure 1B) was able to activate the corresponding QS circuit. In order to advance our understanding of the R protein environment, we dealt with various stereoisomers of the synthetic agonists. Based on our understanding that even small structural changes affect the outcome of activity to a great extent, we reasoned that altering stereochemistry of the synthetic agonists would provide valuable insight into the stereoenvironment of the QS regulators. To further assist in understanding the molecular interaction between synthetic agonists and a QS regulator, LasR, we built an in silico model of the LasR active site based on its homolog protein, TraR, and carried out docking studies for AI analogs. Although the crystal structures for the *P. aeruginosa* QS regulators are currently unavailable, this in silico model of LasR has given us not only better understanding of its molecular interaction with the AI analogs, but also a foundation toward the rational design of novel agonists and antagonists in the future.

Results and Discussion

Synthesis of Enantiomerically Pure AI Analogs

The requisite amino alcohols for the enantiomerically pure form of *trans*-derivatives, (*S,S*)-**1**, (*S,S*)-**2**, (*R,R*)-**1**, and (*R,R*)-**2** (Figure 1C; note that **1** and **2** represent the derivatives of aminocyclohexanol and cyclepentanol, respectively, and that the first stereochemistry with *S* is consistent with that of L-HSL), were synthesized by a known strategy, consisting of a catalytic asymmetric ring opening reaction of cyclohexene oxide and cyclopentene oxide with Jacobsen's catalyst (Figure S1; see the Supplemental Data available with this article online) [17]. The corresponding *cis*-amino alcohols, (*S,R*)-**1**, (*S,R*)-**2**, (*R,S*)-**1**, and (*R,S*)-**2**, were obtained by inversion of the hydroxyl group. These amino alcohols were then coupled with the fatty acid side chains to obtain the desired $3OC_{12}$ and C_4 analogs (Figures S2 and S3).

*Correspondence: hsuga@rcast.u-tokyo.ac.jp

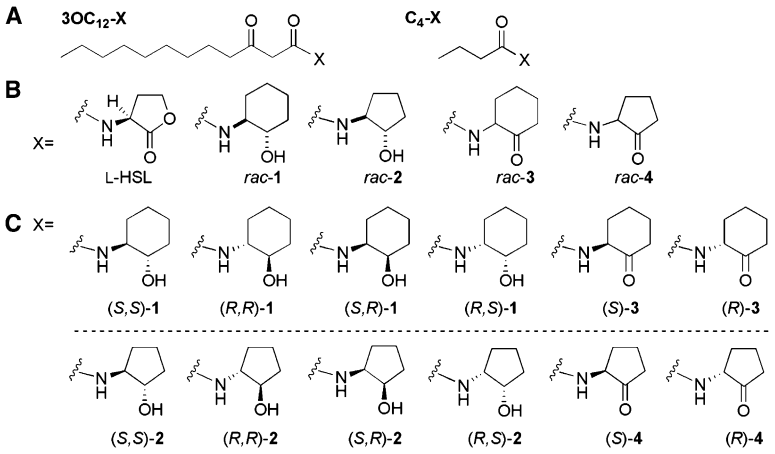

Figure 1. Chemical Structures of the Autoinducer and Autoinducer Analogs

(A) Structure of $3OC_{12}$ and the C_4 side chain.

(B) Natural AI and AI analogs derived from racemic cyclohexanol/one and cyclopentanol/one.

(C) AI analogs derived from enantiomerically pure cyclohexanol/one and cyclopentanol/one.

The 2-aminocycloketone derivatives, (*S*)-**3**, (*R*)-**3**, (*S*)-**4**, and (*R*)-**4** (note that **3** and **4** represent the derivatives of aminocyclohexanone and pentanone, respectively), were synthesized by Dess-Martin oxidation of their hydroxyl derivatives (Figures S2 and S3) [18].

Agonist activity of these derivatives was tested by their ability to induce the expression of green fluorescent protein (GFP) in *P. aeruginosa* reporter strains PAO-JP2 (p*lasI*-LVAgfp), for the $3OC_{12}$ analogs, and PAO-JP2 (p*rhlI*-LVAgfp), for the C_4 analogs [19], in which each QS system can be exogenously activated by the addition of the synthetic AIs or analogs, correlating to the level of GFP expression.

Activation of the *las* Circuit by Amino Alcohol Derivatives

The $3OC_{12}$ derivatives of *trans*-aminocyclohexanol, (*S,S*)-**1** and (*R,R*)-**1**, and *trans*-aminocyclopentanol, (*S,S*)-**2** and (*R,R*)-**2**, were tested for *las* activation. Among these, $3OC_{12}$-(*S,S*)-**1** exhibited the highest activity, which was nearly comparable to the cognate AI, $3OC_{12}$-L-HSL (Figure 2A), while $3OC_{12}$-(*R,R*)-**1** had ~2-fold poorer activity than $3OC_{12}$-(*S,S*)-**1**. These results are predicted to some extent based on the fact that the natural $3OC_{12}$-L-HSL stimulates the *las* circuit more effectively than the unnatural $3OC_{12}$-D-HSL [20]. Despite the predicted stereochemical preference, the observed difference in activity between $3OC_{12}$-L-HSL and $3O_{12}$-D-HSL is much larger than that between derivatives of (*R,R*)-**1** and (*S,S*)-**1** (Figure S5). This indicates that LasR more severely discriminates the stereochemistry of HSL than that of the analog. On the other hand, both stereoisomers of *trans*-aminocyclopentanol were nearly inactive (Figure 2B), suggesting that presentation of the amide and hydroxyl groups in the *trans*-aminocyclopentanol derivatives to the stereoenvironment in the LasR ligand binding site differs from that of the *trans*-aminocyclohexanol derivatives.

Interestingly, LasR responded to the *cis*-isomers with a different stereochemical preference than the *trans*-isomers (Figure 2A). Unlike the observation for the *trans*-isomers of aminocyclohexanol, the (*R,S*)-**1** derivative bearing the opposite stereochemistry to L-HSL showed slightly higher agonist activity than the (*S,R*)-**1** derivative. On the other hand, in the case the *cis*-aminocyclopentanols, $3OC_{12}$-(*S,R*)-**2** shows agonist activity (Figure 2B). This result is prominent since, among the four aminocyclopentanol derivatives tested, only the *(S,R)*-**2** derivative exhibited observable agonist activity at concentrations below 50 μM (Figure S4). Although none of these compounds were as active as $3OC_{12}$-(*S,S*)-**1**, these results seem to indicate that the agonist activity depends on the ring scaffold in which the projection of the amide and hydroxyl groups is appropriate for the interaction with the residues in LasR.

Activation of the *rhl* Circuit by Amino Alcohol Derivatives

The trends for the agonist activity of the C_4-aminocyclohexanol derivatives for the *rhl* circuit correlated with those for the *las* circuit. Among these analogs, only C_4-(*S,S*)-**1** exhibits significant agonist activity, and others show modest (C_4-(*R,S*)-**1**) or poor activity (Figure 2C). Two noteworthy observations were made in this series of studies for the cyclohexanol derivatives. First, this study has revealed that C_4-(*S,S*)-**1** acts as an effective *rhl* agonist, whereas its enantiomer, C_4-(*R,R*)-**1**, is a poor agonist. The observed difference in activity between these two C_4 *trans*-enantiomers is more pronounced than that between $3OC_{12}$ *trans*-enantiomers (Figure 2C versus Figure 2A), somewhat similar to the observation of $3OC_{12}$-L-HSL versus $3OC_{12}$-D-HSL [20]. Second, in the case of *cis*-isomers, C_4-(*R,S*)-**1** is modest but clearly active, while C_4-(*S,R*)-**1** is inactive, in contrast to the observed trend of their *trans*-derivatives as discussed above. Thus, it is clear that, in the case of *cis*-cyclohexanol derivatives, those with the reversed stereochemistry of the amide group show higher activity than the natural configuration.

We also synthesized and tested a series of C_4-aminocyclopentanol derivatives, stereoisomers of C_4-**2**, for the *rhl* circuit activation (Figure 2D). These four stereoisomers exhibited modest, but a somewhat similar degree of, *rhl* agonist activity. This is in sharp contrast to the observation that $3OC_{12}$-**2** derivatives exhibited a significant difference in the ability to activate the *las* circuit, in which three out of four molecules are inactive (Figure 2B).

Activation of *las* and *rhl* Circuits by Amino Ketone Derivatives

Lastly, a set of AI analogs consisting of amino ketone derivatives **3** and **4** was tested. Neither the $3OC_{12}$

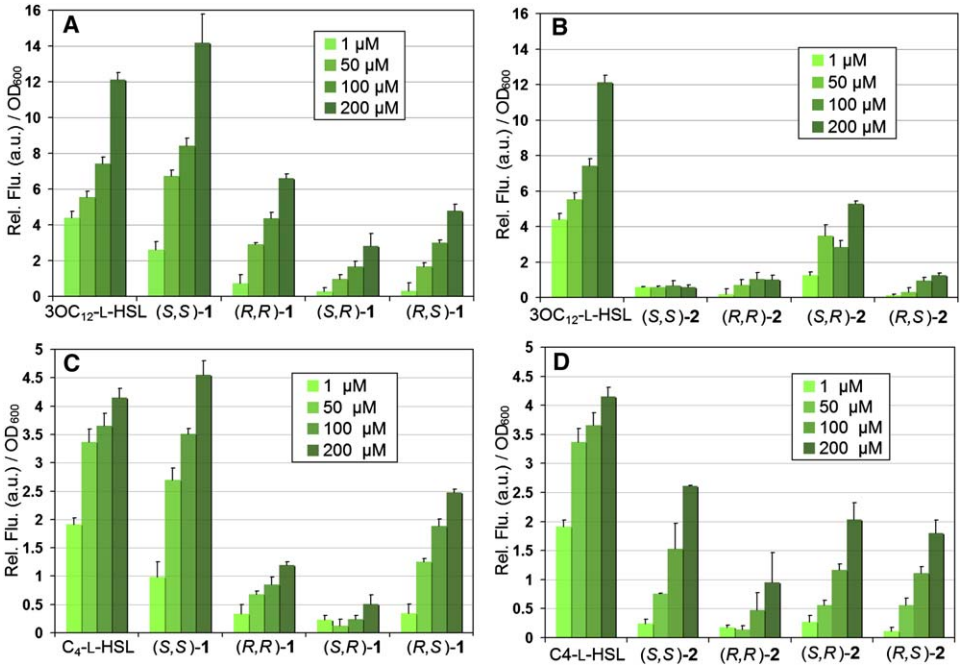

Figure 2. Agonist Activity of Cyclohexanol and Pentanol Derivatives

(A–D) (A) $3OC_{12}$-cyclohexanol derivatives for the *las* circuit. (B) $3OC_{12}$-cyclopentanol derivatives for the *las* circuit. (C) C_4-cyclohexanol for the *rhl* circuit. (D) C_4-cyclopentanol derivatives for the *rhl* circuit. The level of GFP expression (relative fluorescence [a.u.]) was monitored by using a molecular imager and was normalized to cell density by dividing the optical density (OD) at a wavelength of 600 nm. The standard deviation was derived from results of four independent experiments. Assays for the *las* circuit, shown in (A) and (B), were carried out in the presence of varying concentrations of the AI analogs, and those for the *rhl* circuit, shown in (C) and (D), were carried out in the presence of 1 μM $3OC_{12}$-L-HSL as well as varying concentrations of the AI analogs. The middle of the error bar shown in each bar represents the mean score from four independent experiments, and the error bar represents the standard deviation of all trials.

derivatives of (*S*)/(*R*)-**3** nor (*S*)/(*R*)-**4** agonize the *las* circuit effectively (Figure 3A). In striking contrast, C_4 derivatives of the cyclic ketones exhibit high agonist activity (Figure 3B), and this activity is dominated by the (*S*)-stereoisomers. With these observations, it is clear that the *S* configuration of the amide group in the C_4-cyclic ketones plays a dominant role in exhibiting agonist activity.

The above-described observations suggest that though the HSL moiety of AIs is the common recognition element for both LasR and RhlR, the microenvironment of the binding site likely differs between LasR and RhlR. With this in mind, the similar conclusion can also be derived from the observed difference in the studies of the aminocyclopentanol derivatives and their cognate circuits (Figure 2B versus Figure 2D); $3OC_{12}$-(*S,S*)-**2** does not stimulate the *las* circuit at any concentration, whereas C_4-(*S,S*)-**2** shows observable activity in the stimulation of the *rhl* circuit. Moreover, LasR is only active toward $3OC_{12}$-(*S,R*)-**2**; however, RhlR exhibits activity toward C_4-(*S,R*)-**2** and C_4-(*R,S*)-**2** at a similar level. All of these results consistently suggest that despite the fact that both LasR and RhlR recognize the HSL moiety

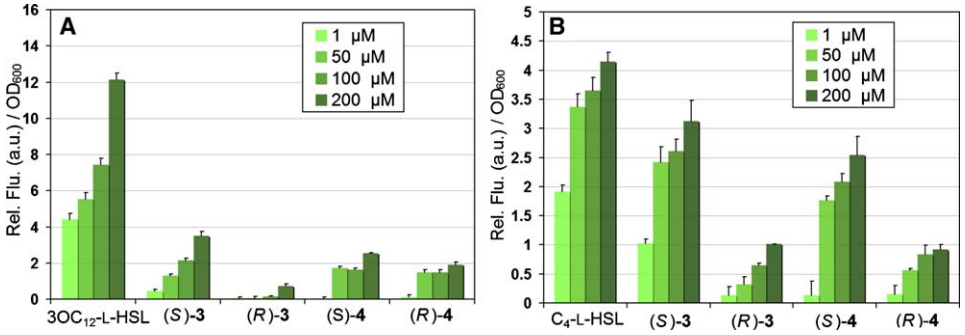

Figure 3. Agonist Activity of Cyclic Ketone Derivatives

(A and B) (A) $3OC_{12}$-cyclohexanone derivatives for the *las* circuit. (B) C_4-cyclohexanone for the *rhl* circuit. Assays for the *las* circuit, shown in (A), were carried out in the presence of varying concentrations of the AI analogs, and those for the *rhl* circuit, shown in (B), were carried out in the presence of 1 μM $3OC_{12}$-L-HSL as well as varying concentrations of the AI analogs. The middle of the error bar shown in each bar represents the mean score from four independent experiments, and the error bar represents the standard deviation of all trials.

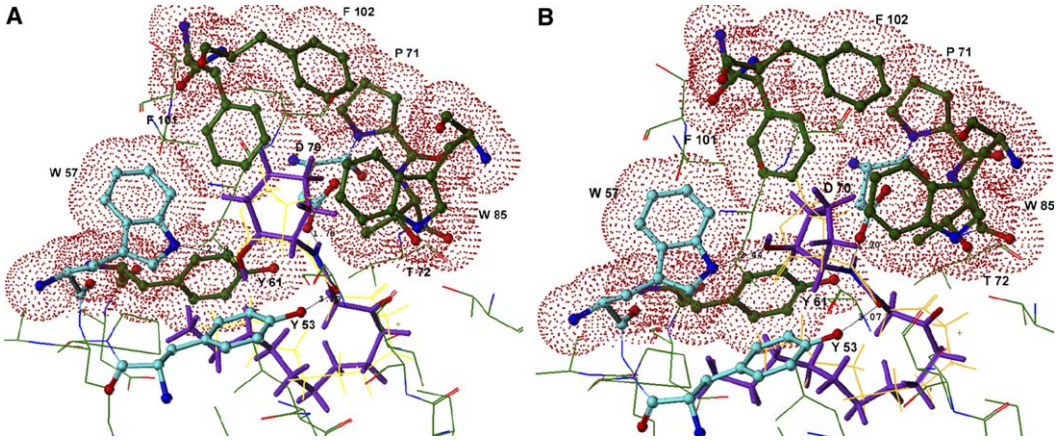

Figure 4. In Silico Model for the Complex of LasR and Agonists

(A and B) (A) 3OC$_{12}$-(*S,S*)-**1** and (B) 3OC$_{12}$-(*S,S*)-**2** were docked to the modeled LasR ligand binding site. Docking was carried out by using the FlexX program on the SYBYL interface. The residues displayed as balls-and-sticks are those involved in hydrogen bonding interactions (Y53, W57, and D70; shown in blue) and those constituting the hydrophobic pocket (Y61, P71, T72, W85, F101, and F102; shown in green). The hydrophobic core is rendered as dots. The analogs (shown as capped sticks in violet) are superimposed over the structure of 3OC$_{12}$-L-HSL (yellow line). Other residues in the ligand binding site are shown as green lines. The docked structures of 3OC$_{12}$-L-HSL and 3OC$_{12}$-(*S,R*)-**2** are included in the Supplemental Data.

of the cognate AIs, the microenvironment of their binding sites is unlikely the same.

Docking Studies for the Natural AI and Its Analogs for the *las* Circuit

In order to examine whether the observed activities of the AI analogs correlated to their ability for accommodation to the ligand binding site, we decided to build an in silico model of the ligand binding site. The screening method utilizing the GFP reporter strain allowed for rapid screening of the analogs for the activation of their respective QS circuits, and docking these analogs in the modeled binding site would provide an understanding of their interactions with the microenvironment at the ligand binding site. We based our model on the available crystal structure of TraR (PDB code: 1L3L) from *Agrobacterium tumefaciens* complexed with its AI and DNA [21, 22], the only available structure of a LuxR homolog. Neither isolation nor expression of active LasR or RhlR has been successful so far. Therefore, these are the only structural data that allow us to build virtual structures of the *P. aeruginosa* R proteins.

TraR AI, 3OC$_8$-HSL with a 3-oxo group, is structurally more similar to LasR AI, 3OC$_{12}$-L-HSL with a 3-oxo group, than to RhlR AI, C$_4$-L-HSLwithout a 3-oxo group. We therefore speculated that the docking studies of LasR-agonist pairs would give us a more reliable prediction for the interaction of the residues with HSL or its analog, and we chose the LasR-agonist pairs for the docking studies. Based on protein sequence alignment of LasR and TraR with ClustalW (Table S1 and Figure S6) [23], the amino acid residues in TraR were replaced with the appropriate ones to construct the in silico model for the LasR AI binding site (Figure S7C). The ligands were docked into the modeled site by using FlexX [24] as the docking program, and scores were computed.

The docking results correlated well with our experimental data (Figures S7A and S7B). The study comparing the activity of the *trans*-aminocyclohexanol and *trans*-aminocyclopentanol derivatives indicated that some additional factor other than stereochemistry played a role in the higher activity of (*S,S*)-**1**, compared to no activity in the case of (*S,S*)-**2** (Figure 4A versus Figure 4B). Docking suggested that, in the case of (*S,S*)-**1**, the cyclohexyl ring deeply penetrates in the hydrophobic pocket, and that the hydroxyl group of (*S,S*)-**1** maintains a hydrogen bonding interaction similar to that of the carbonyl group of HSL (see also Figure S7C). A combination of the hydrophobic contacts and a hydrogen bonding interaction probably make 3OC$_{12}$-(*S,S*)-**1** a strong agonist. The lesser activity of the opposite stereoisomer, 3OC$_{12}$-(*R,R*)-**1**, can be explained based on the fact that, though the hydrophobic contacts are maintained, the hydroxyl group flips to the opposite side upon accommodation of the reversed stereogenic center to the ligand binding site (data not shown). In the case of 3OC$_{12}$-(*S,S*)-**2**, it appears that the placement of the cyclopentyl ring in a slightly tilted position relative to the HSL ring might serve to maintain the hydrogen bonding interactions with W57 (Figure 4B). This may result in loss of interactions with the hydrophobic surface and therefore loss of the agonist activity. Thus, it seems that hydrophobic contacts contribute to a greater extent in governing the activity.

Next, the explanation for the activity of the *cis*-isomer, 3OC$_{12}$-(*S,R*)-**2**, compared to the inactive *trans*-isomer, 3OC$_{12}$-(*S,S*)-**2**, was sought. Docking of 3OC$_{12}$-(*S,R*)-**2** to the ligand binding site showed that the cyclopentyl ring penetrates the hydrophobic pocket in a manner similar to that observed for 3OC$_{12}$-(*S,S*)-**1** (Figure S7C versus Figure S7D), compared to the tilted accommodation of 3OC$_{12}$-(*S,S*)-**2** (Figure 4B). The modest activity of 3OC$_{12}$-(*S,R*)-**2** is probably due to the extended distance and hence the weakened hydrogen bonding interaction between the hydroxyl group and W57.

Our docking studies agreed well with the experimental data (Figures S7A and S7B), but a shortcoming of our approach should also be mentioned. Since the

predocking LasR structure was generated by in silico mutations of a homolog protein (TraR) as described (Table S1 and Figure S6), the hydrophobic interactions in the fatty acid binding site consisting of many of these residues could not be well defined. Because of this unknown contribution from such ambiguously defined interactions to ligand binding, we intentionally excluded them from the free energy estimation. However, since all agonists share the same 3O-C_{12} fatty acid chain, and since positioning of the amide group was not drastically different among the docking models, we believe that our simulations could generate a meaningful explanation of the observed strength of agonist binding.

In conclusion, our docking studies gave us critical insight into the LasR-agonist interaction. The combination of the hydrophobic interaction of the hydrocarbon ring and hydrogen bonding interaction with the hydroxyl group on the ring is a critical determinant for agonist activity. $3OC_{12}$-(*S,S*)-**1** acts as a strong agonist, because both interactions are maintained better than the other two analogs tested for the docking studies. Its cyclohexyl ring deeply penetrates into the hydrophobic pocket to maximize the hydrophobic interaction, and, also, the (*S,S*)-stereochemistry of the hydroxyl and amide groups allows for maintenance of the hydrogen bonding with W57, D70, and Y53. Based on the results observed for the aminoacyclopentanol derivatives, we suggest that the extended hydrophobic interaction plays a more crucial role in binding than the hydrogen bonding interaction with W57. Such information would be useful for rational design of molecules that antagonize the QS circuits in the future.

Significance

The key for designing antagonists for the QS regulators lies in understanding the regulatory protein environment. With this intention, we probed the protein environment with a series of enantiomerically pure derivatives of the autoinducer analogs. One of the striking findings here is that, depending on the ring structure, the appropriate combination of absolute and relative stereochemistries of the amide and hydroxyl groups dictates the exhibition of agonist activity. In addition, the docking studies shed light on the contribution of the hydrophobic residues and specific hydrogen bonding interactions in determining the outcome of activity. The inputs gained from this study would provide both stereochemical and structural considerations for the design of potent agonists and antagonists.

Experimental Procedures

Abbreviations

$LiOH{\bullet}H_2O$, lithium hydroxide monohydrate; THF, tetrahydrofuran; EDCI, 1-(3-dimethylaminopropyl)-3-ethyl-carbodiimidehydrochloride; DMAP, dimethylamino-pyridine; L-HSL, L-homoserine lactone; DMF, dimethyl formamide; iPr$_2$NEt, diisopropylethylamine; TEA, triethylamine; *n*-BuLi, *n*-butyl lithium; *p*-TsOH, *p*-toluene sulphonic acid; TFA, trifluroacetic acid.

Synthesis of the Natural Autoinducers

The natural AIs, $3OC_{12}$-L-HSL and C4-L-HSL, were prepared according to published procedures. All analytical data were consistent with those in the literature.

Synthesis of 2-Amino Cyclic Alcohols

2-Amino cyclic alcohols ((*S,S*)-**1**, (*S,R*)-**1**, (*R,R*)-**1**, (*R,S*)-**1**, (*S,S*)-**2**, (*S,R*)-**2**, (*R,R*)-**2**, and (*R,S*)-**2**) were prepared according to published procedures, as shown in Figure S1. The analytical data for all intermediate and final compounds were consistent with those in the literature.

Synthesis of Autoinducer Analogs

General Synthetic Procedures of $3OC_{12}$ Derivatives of 2-Aminocyclohexanol or Pentanol

3,3-ethylenedioxydodeca-noic acid (see Figure S2) was prepared according to the procedures previously reported [7]. It was then coupled with the corresponding 2-aminocyclohexanol ((*S,S*)-**1**, (*S,R*)-**1**, (*R,R*)-**1**, or (*R,S*)-**1**) or 2-aminocyclopentanol ((*S,S*)-**2**, (*S,R*)-**2**, (*R,R*)-**2**, or (*R,S*)-**2**) in the presence of EDCI, DMAP, and iPr$_2$EtN in DMF according to the procedures previously reported. The obtained molecule was treated with TFA in CH_2Cl_2 to remove the cyclic ketal protective group, followed by purification on silica gel, resulting in the desired AI analogs in an ~75%–85% yield. All characterizations are included in the Supplemental Data. See more detailed procedures in [14] and [15].

General Synthetic Procedures of $3OC_{12}$ Derivatives of 2-Aminocyclohexanone or Pentanone

N-[2-hydroxycyclohexyl]-(3,3-ethylenedioxy)-dodecanamide was treated with 1.1 equivalents of Dess-Martin periodinane in CH_2Cl_2 [18], followed by TFA deprotection to give the desired $3OC_{12}$ derivatives of (*S*)- or (*R*)-2-aminocyclohexanone or pentanone in an ~65%–75% yield (Figure S2). See more detailed procedures in [14] and [15].

General Synthetic Procedures of C_4 Derivatives of 2-Aminocyclohexanol or Pentanol and 2-Aminocyclohexanone or Pentanone

Butyryl chloride was coupled with the corresponding 2-aminocyclohexanol or pentanol to give the C4 derivative of (*S,S*)-**1**, (*S,R*)-**1**, (*R,R*)-**1**, (*R,S*)-**1**, (*S,S*)-**2**, (*S,R*)-**2**, (*R,R*)-**2**, or (*R,S*)-**2**, according to the procedures previously reported (yield of 80%–85%) (Figure S3). The C_4-amino alcohol derivatives were treated with Dess-Martin periodinane to give the desired cyclic ketone derivatives in an ~70%–75% yield.

Procedure for Reporter Strain Assays

The reporter strains PAO-JP2 (p*lasI*-LVAgfp) and PAO-JP2 (p*rhlI*-LVAgfp) were grown overnight in CIRCLEGROW (Bio101, Inc.) media containing 300 μg/ml and 100 μg/ml carbenicellin, respectively, at 37°C and were diluted to an OD_{600} of 0.1. After incubation for 1 hr, 200 μl cell culture was added to individual wells of a 96-well plate containing the desired analogs to be tested. All derivatives and synthetic autoinducers were added to wells as solutions in chloroform; the wells were thoroughly dried before addition of cell culture. For the *las* circuit, concentrations ranging from 1 to 200 μM $3OC_{12}$-L-HSL were added in the control wells. The individual analogs were added to separate wells in the same concentration range. For the *rhl* circuit, control wells consisted of 1 μM $3OC_{12}$-L-HSL in addition to varying concentrations of C4-L-HSL ranging from 1 to 200 μM. In the test wells, individual analogs were added to separate wells along with 1 μM $3OC_{12}$-L-HSL. The plates were incubated for 6 hr with shaking at 37°C and were scanned for fluorescence emission by using a BIORAD Molecular Imager (488 nm excitation and 695 nm bandpass filter). The level of GFP expression (relative fluorescence [a.u.]) was quantified by using ImageQuant software and was normalized to cell density by dividing the optical density (OD) at a wavelength of 600 nm. The standard deviation was derived from results in four independent experiments.

Supplemental Data

Supplemental Data including figures for synthesis, characterizations, experimental details for a reporter strain assay, a table of modified residues for the LasR model, and docking studies for $3OC_{12}$-L-HSL and its analogs are available at http://www.chembiol.com/cgi/content/full/13/2/123/DC1/.

Acknowledgments

We thank Dr. Y. Bu for earlier effort toward this work. We also thank Drs. R. Cheng and D. Hangauer for the discussion of computer modeling experiments. This work was supported by the Product

Development Award at UB and Discovery Research, and it was partly funded by Otsuka Chemical Co., Ltd.

Received: April 18, 2005
Revised: October 28, 2005
Accepted: December 2, 2005
Published: February 24, 2006

References

1. Oliver, A., Cantón, R., Campo, P., Baquero, F., and Blázquez, J. (2000). High frequency of hypermutable *Pseudomonas aeruginosa* in cystic fibrosis lung infection. Science *288*, 1251–1253.
2. Passador, L., Cook, J.M., Gambello, M.J., Rust, L., and Iglewski, B.H. (1993). Expression of Pseudomonas aeruginosa virulence genes requires cell-to-cell communication. Science *260*, 1127–1130.
3. Van Delden, C., and Iglewski, B. (1998). Cell-to-cell signaling and *Pseudomonas aeruginosa* infections. Emerg. Infect. Dis. *4*, 1–13.
4. Fuqua, C., and Greenberg, E.P. (2002). Listening in on bacteria: acyl-homoserine lactone signaling. Nat. Rev. Mol. Cell Biol. *3*, 685–695.
5. Miller, M.B., and Bassler, B.L. (2001). Quorum sensing in bacteria. Annu. Rev. Microbiol. *55*, 165–199.
6. Singh, P.K., Schaefer, A.L., Parsek, M.R., Moninger, T.D., Welsh, M.J., and Greenberg, E.P. (2000). Quorum-sensing signals indicate that cystic fibrosis lungs are infected with bacterial biofilms. Nature *407*, 762–764.
7. Pearson, J.P., Gray, K.M., Passador, L., Tucker, K.D., Eberhard, A., Iglewski, B.H., and Greenberg, E.P. (1994). Structure of the autoinducer required for expression of *Pseudomonas aeruginosa* virulence genes. Proc. Natl. Acad. Sci. USA *91*, 197–201.
8. Pearson, J.P., Passador, L., Iglewski, B.H., and Greenberg, E.P. (1995). A second *N*-acyl-homoserine lactone signal produced by *Pseudomonas aeruginosa*. Proc. Natl. Acad. Sci. USA *92*, 1490–1494.
9. Latifi, A., Foglino, M., Tanaka, K., Williams, P., and Lazdunski, A. (1996). A hierarchical quorum-sensing cascade in *Pseudomonas aeruginosa* links the transcriptional activators LasR and RhlR (VsmR) to expression of the stationery-phase sigma factor RpoS. Mol. Microbiol. *21*, 1137–1146.
10. Pearson, J.P., Pesci, E.C., and Iglewski, B.H. (1997). Roles of *Pseudomonas aeruginosa las* and *rhl* quorum-sensing systems in control of elastase and rhamnolipid biosynthesis genes. J. Bacteriol. *179*, 5756–5767.
11. Pearson, J.P., Feldman, M., Iglewski, B.H., and Prince, A. (2000). *Pseudomonas aeruginosa* cell-to-cell signaling is required for virulence in a model of acute pulmonary infection. Infect. Immun. *68*, 4331–4334.
12. Tang, H.B., DiMango, E., Bryan, R., Gambello, M., Iglewski, B.H., Goldberg, J.B., and Prince, A. (1996). Contribution of specific *Pseudomonas aeruginosa* virulence factors to pathogenesis of pneumonia in a neonatal mouse model of infection. Infect. Immun. *64*, 37–43.
13. Suga, H., and Smith, K.M. (2003). Molecular mechanisms of bacterial quorum sensing as a new drug target. Curr. Opin. Chem. Biol. *7*, 586–591.
14. Smith, K.M., Bu, Y., and Suga, H. (2003). Library screening for synthetic agonists and antagonists of a *Pseudomonas aeruginosa* autoinducer. Chem. Biol. *10*, 563–571.
15. Smith, K.M., Bu, Y., and Suga, H. (2003). Induction and inhibition of *Pseudomonas aeruginosa* quorum sensing by synthetic autoinducer analogs. Chem. Biol. *10*, 81–89.
16. Fast, W. (2003). Molecular radio jamming: autoinducer analogs. Chem. Biol. *10*, 1–2.
17. Schaus, S.E., Larrow, J.F., and Jacobsen, E.N. (1997). Practical synthesis of enantiopure cyclic *1*, 2-amino alcohols via catalytic ring opening of meso epoxides. J. Org. Chem. *62*, 4197–4199.
18. Dess, D.B., and Martin, J.C. (1991). A useful 12-I-5 triacetoxyperiodinane (the Dess-Martin periodinane) for the selective oxidation of primary or secondary alcohols and a variety of related 12-I-5 species. J. Am. Chem. Soc. *113*, 7277–7287.
19. De Kievit, T., Gillis, R.J., Marx, S., Brown, C., and Iglewski, B.H. (2001). Quorum-sensing genes in *Pseudomonas aeruginosa* biofilms: their role and expression patterns. Appl. Environ. Microbiol. *67*, 1865–1873.
20. Ikeda, T., Kajiyama, K., Kita, T., Takiguchi, N., Kuroda, A., Kato, J., and Ohtake, H. (2001). The synthesis of optically pure enantiomers of N-acyl-homoserine lactone autoinducers and their analogues. Chem. Lett. (Jpn.) *30*, 314–315.
21. Zhang, R.-G., Pappas, T., Brace, J., Miller, P.C., Oulmassov, T., Molyneaux, J.M., Anderson, J.C., Bashkin, J.K., Winans, S.C., and Joachimiak, A. (2002). Structure of bacterial quorum-sensing transcription factor complexed with phermone and DNA. Nature *417*, 971–974.
22. Vannini, A., Volpari, C., Gargioli, C., Muraglia, E., Cortese, R., De Francesso, R., Neddermann, P., and Di Marco, S. (2002). The crystal structure of the quorum sensing protein TraR bound to its autoinducer and target DNA. EMBO J. *21*, 4393–4401.
23. Thompson, J.D., Higgins, D.G., and Gibson, T.J. (1994). Clustal W: improving the sensitivity of progressive multiple sequence alignment through sequence weighting, position-specific gap penalties and weight matrix choice. Nucleic Acids Res. *22*, 4673–4680.
24. Rarey, M., Kramer, B., Lengauer, T., and Klebe, G. (1996). A fast flexible docking method using an incremental construction algorithm. J. Mol. Biol. *261*, 470–489.

Accession Numbers

Coordinates for TraR have been deposited in the Protein Data Bank with accession code 1L3L.